QIRT 2018
10.21611/qirt.2018.102
14th Quantitative InfraRed Thermography Conference

# Active Thermography with frequency modulated source

by P. Bison[1], A. Bortolin[1], G. Cadelano[1], G. Ferrarini[1], L. Finesso[2]

[1]CNR-ITC, Corso Stati Uniti 4, 35127 Padova, Italy paolo.bison@itc.cnr.it
[2] IEIIT-CNR, via Gradenigo 6/B - 35131, Padova, Italy.

**Abstract**

Active Infrared Thermography is applied on a CFRP slab, prepared with teflon inserts of various dimensions and located at different depths, to simulate the presence of defects inside the material. The aim is that of comparing the pulse, the periodically modulated, the chirp methods of heating. Each heating method will be presented together with the description of the adopted signal processing algorithm.

## 1. Introduction

Active Infrared Thermography is a technique widely used in assessing the conditions of parts of industrial components. It consists in the generation of heat in the component under test and in monitoring by InfraRed Thermography (IRT) the time evolution of the surface temperature. The heat generation can be done by several techniques (hot air, induction, acoustic waves etc.). Nonetheless the photothermal one is by far the most used consisting in the generation of heat as a consequence of the absorption of electromagnetic waves, typically (even though not necessarily) in the visible band. Lamps delivering either a flash pulse or a periodically modulated light are the most commonly used methods of heating. In both cases thermography records the time evolution of the surface temperature of the heated part. For pulse, data are successively treated according to various algorithms: among them Pulse Phase Thermography (PPT) [1], Principal Component Thermography (PCT) [2], Thermographic Signal Reconstruction (TSR) [3], Thermal Tomography (TT) [4] etc. For periodically modulated source the data processing follows in some way what is done by a lock-in amplifier [5,6]. In the past the scientific community working in the field of IRT had been speculating on the best heating method to adopt (according to some optimum criterion) in such a way to increase as much as possible the detectability of inner defects [7,8]. More recently, a new heating method has been proposed: It appears as a trade off between the pulse and periodic heating methods. It consists in the frequency modulation of the heating source by means of a chirp signal in one case, and in the application of suitable on-off sequence to a lamp according to the Barker code [9-15], the digital version of the chirp signal. Both heating schemes derive from the signal processing strategies adopted in the Radar technology.

The aim of this paper is that of comparing the pulse, the periodically modulated, the chirp methods of heating. The three methods will be applied on a CFRP slab, prepared with teflon inserts of various dimensions and located at different depths, to simulate the presence of defects inside the material. The maps are prepared to be statistically evaluated in terms of sensitivity and specificity [16] by comparison with the 'true' map of the defects. This statistical evaluation will be faced in a future work. Each heating method will be presented together with the description of the adopted signal processing algorithm.

## 2. Experimental layout

The experimental layout is sketched in Figure 1. According to the Thermal NonDestructive Testing reflection scheme the specimen is heated on the side of interest and the temperature is measured on the same side. Usually a sequence of images is collected and analysed. Test duration and frame rate depends on the type of heating function adopted.

10.21611/qirt.2018.102


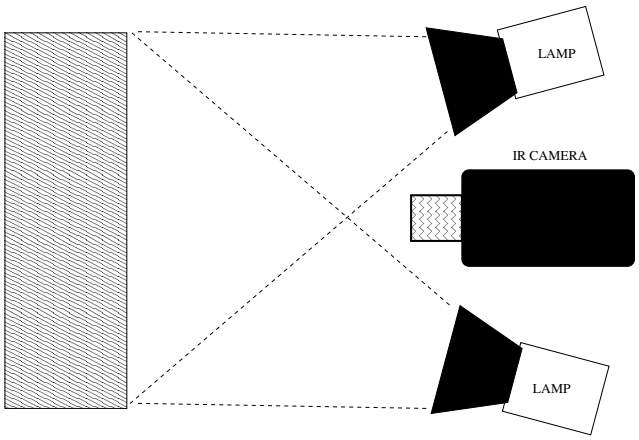


*Fig. 1. Experimental layout for reflection scheme: heating source and detector are on the same side of the sample to test. The lamps are either flash xenon discharge lamps 2.4 kJ or halogen type with maximum power 1 kW each. They are supplied by a capacitor pack in the former case and a power thyristor unit Eurotherm 7100, driven by a NI 6110 general purpose I/O box connected to a computer by USB in the latter. IR camera is a FLIR SC 3000, QWIP detector, 320 X 240 pixels @ 50Hz, 8 to 9 $\mu$m wavelenght band.*

The comparison of the effectiveness of the kind of heating function and the related data reduction scheme is done on a specimen of CFRP with teflon inserts artificially introduced in between successive plies to simulate the presence of delaminations of different size and at diffrent depths. The scheme of the specimen is reported on Figure 2. In Figure 3 a binary map of the same dimension of the image produced by the thermographic camera is produced. This binary image can be utilized to check the effectiveness of the detection procedure (heating function plus data reduction algorithm) by comparison with the binary result of the process obtained by suitable thresholding.

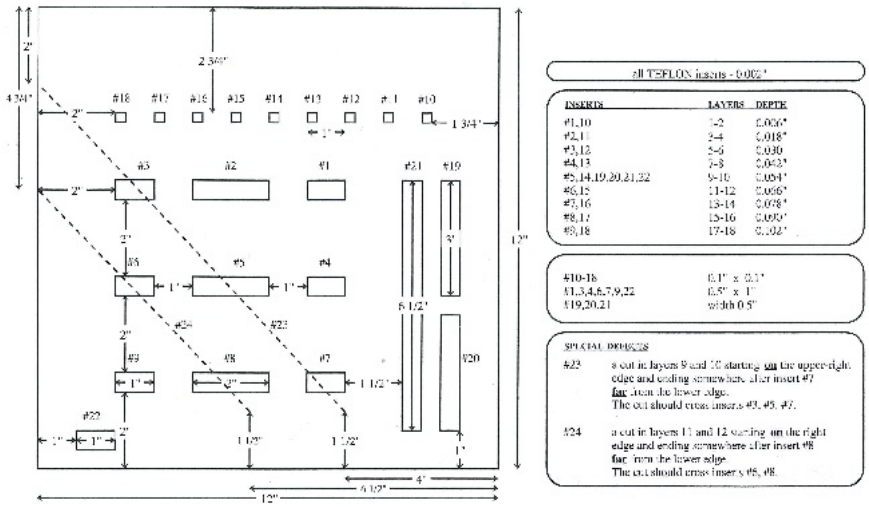


*Fig. 2. Scheme of the position, dimension and depth of the teflon inserts positioned in CFRP specimen to simulate the presence of delaminations.*

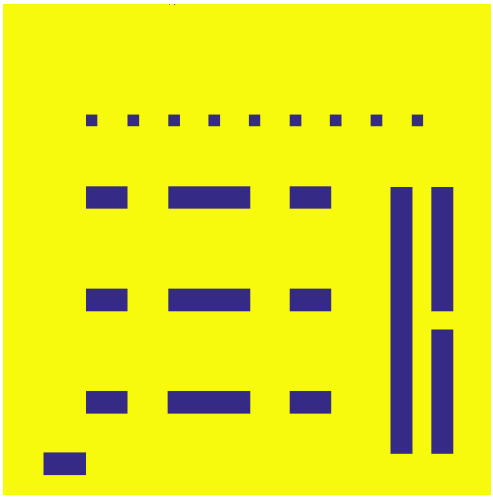

*Fig. 3. Binary image of the spatial location and dimension of the defect inserted in CFRP specimen. Its dimension are directly comparable to the result obtained by processing the images of the thermographic camera as it is characterized by the same geometric resolution.*

## 3. Heating functions and processing algorithms

According to the heating function adopted, one or more data reduction schemes have been applied to highlight the presence of defects in the tested specimen.

### Pulse heating

Following the scheme shown in Figure 1, the lamps deliver a short powerful pulse of light with a duration of some milliseconds. Specifically, a photographic flash system is utilized with 2 lamps, 2.4 kJ each. The pulse duration is around 5 ms. The typical temperature profile collected by the IR camera, refered to the initial (ambient) temperature is shown in Figure 4, for a sound area (blue color) and a defected one (red color). The initial time (t=0) corresponds to the delivering of the pulse.

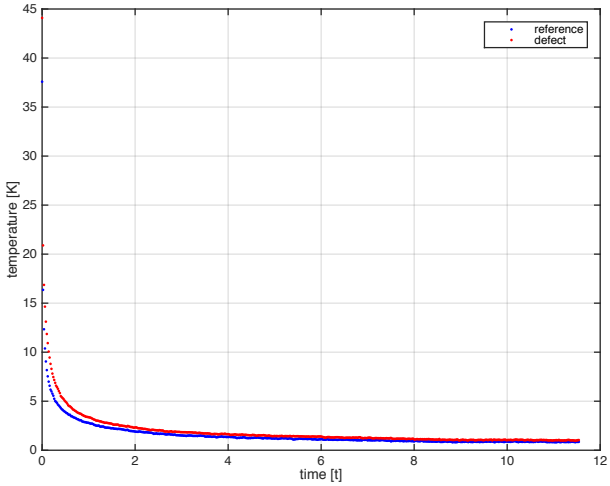


*Fig. 4. Temperature profiles collected after the release of the pulse in correspondence of a sound (reference) zone in blue and a defect zone in red.*

#### *3.1.3. Pulse Phase Thermography*

According to PPT the temperature profile shown in Figure 4 have been processed by applying the Fast Fourier Transform. The results are shown in Figure 5 where the amplitude and phase as a function of frequency are presented.

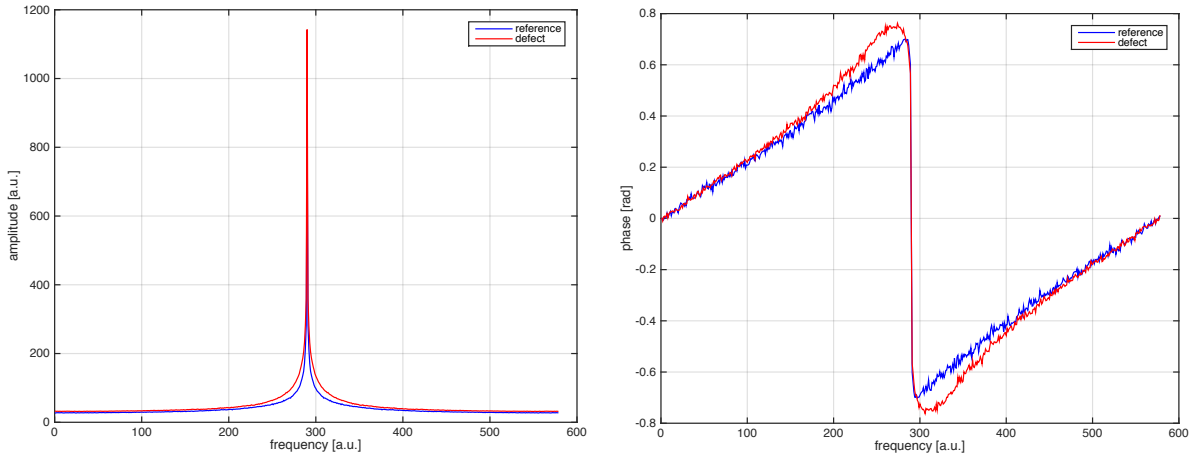


*Fig. 5. On the left the amplitude and on the right the phase obtained after processing the profiles of Figure 4 by Fast Fourier Transform algorithm.*

By applying the the FFT to each pixel in the sequence of images the maps shown in Figure 6 are obtained. The frequency selected for the maximum contrast between backgroud (sound areas) and defects is 0.087 Hz.

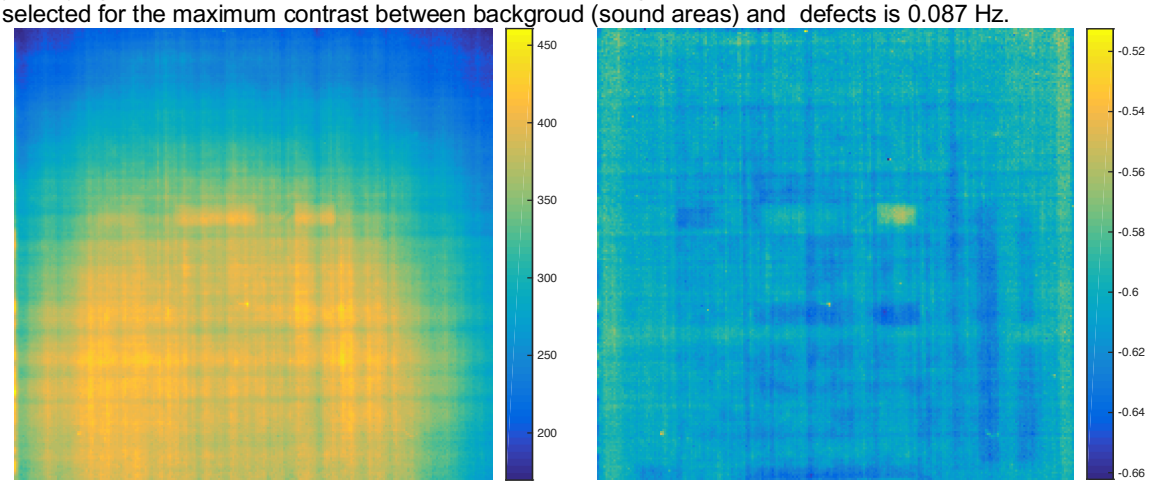

*Fig. 6. Amplitude (left) and phase (right) maps obtained by processing pixel by pixel the IR sequence with FFT algorithm.*

### *3.1.3. Thermographic Signal Reconstruction*

The profiles shown in Figure 4 can be as well processed by taking the logarithm of the temperature and time and successively fitting the data by a polynomial function. That allows for an easy evaluation of the first and second derivatives whose results are shown in Figure 7.

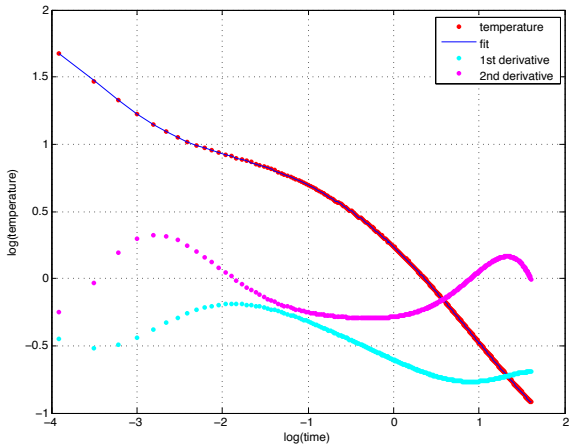


*Fig. 7. Temperature vs time after log-log transformation. The defect behaviour is shown together with the polynomial fitting function and the first and second derivative.*

By applying the TSR algorithm to each pixel in the sequence of images, the maps shown in Figure 8 are obtained. The maximum and minimum of first (D1) and second (D2) derivatives are shown.

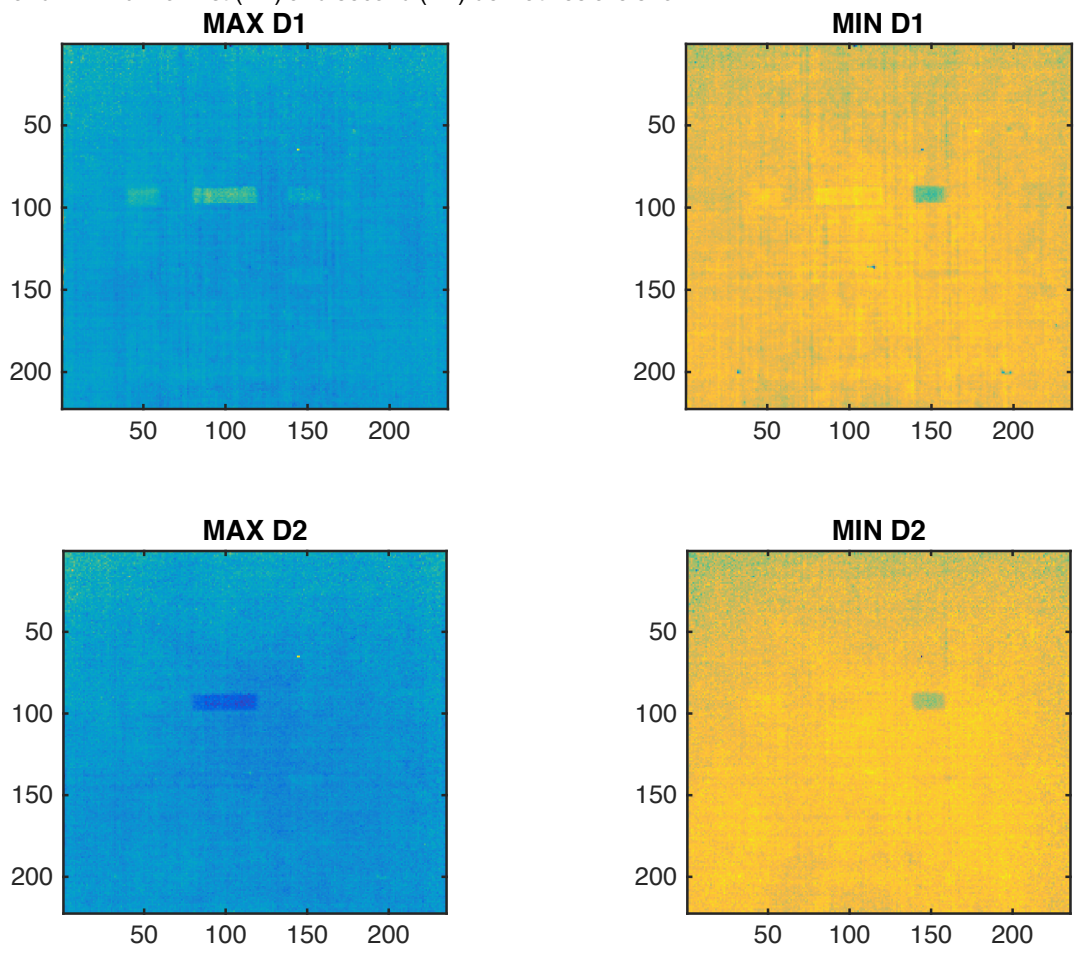


*Fig. 8. Maximum (left) and Minimum (right) of the first (D1) and second (D2) derivatives of the log-log fitting polynomial function.*

### *3.1.3. Principal Component Thermography*

This statistical algorithm is obtained after flattening the original 3D data structure (x, y, t) by rearranging each image of the sequence in a vector of dimension x·y and by stacking each vector to form a new matrix of dimensions (t, x·y). The covariance of this new matrix is computed and its eigenvalue equation is solved. The eigenvalues and eigenvectors are shown in Figure 9.

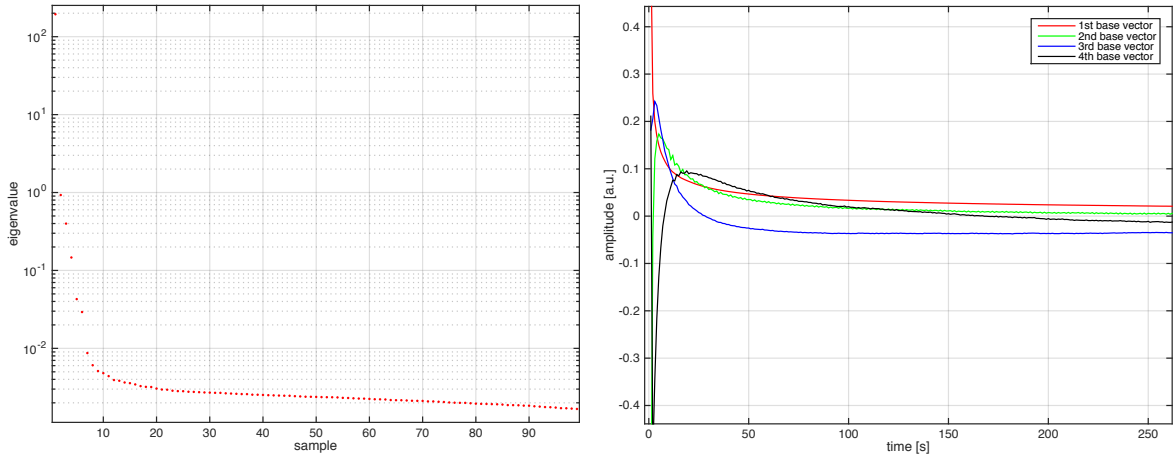


*Fig. 9. First Eigenvalues (left) and eigenvectors (right), solution of the eigenvalue equation for the covariance matrix obtained after suitable flattening of the original 3D data matrix.*

By projecting the original data on the principal eigenvectors the images of Figure 10 are obtained.

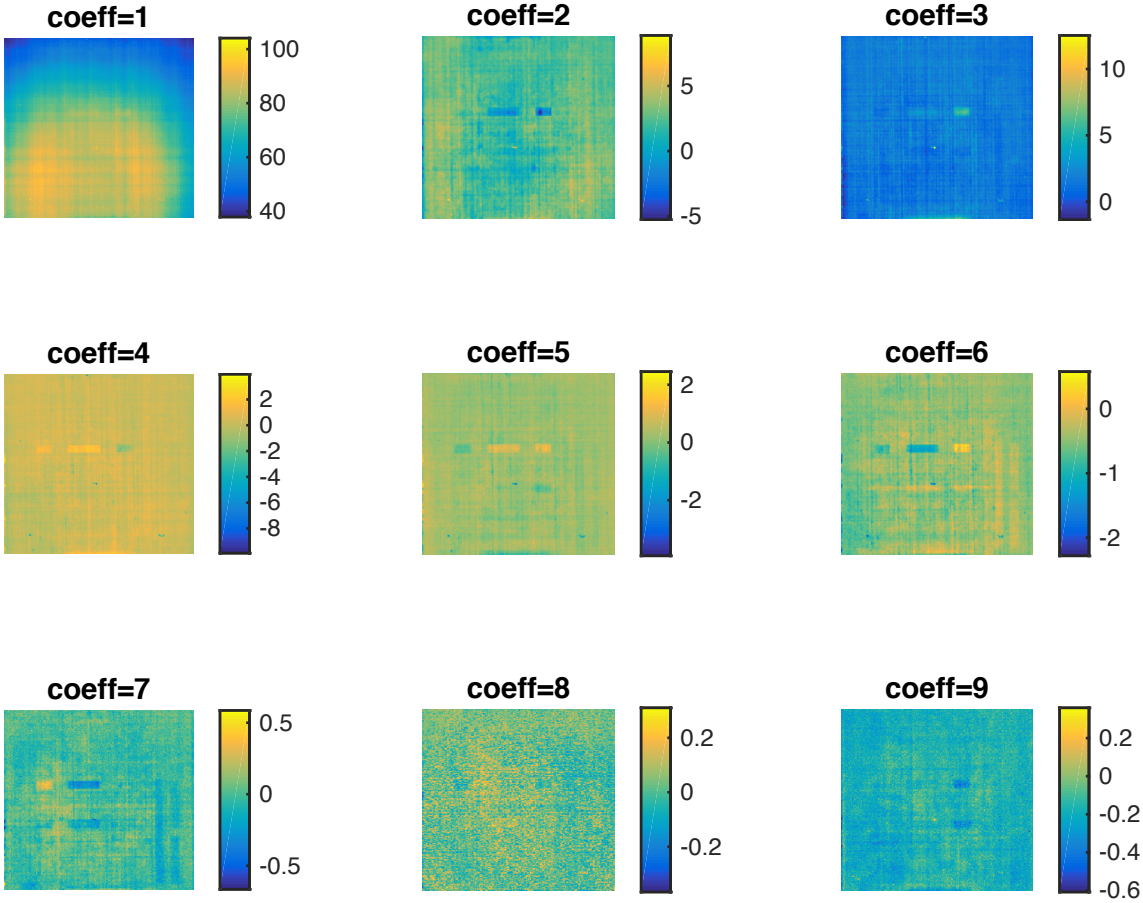


*Fig. 10. The projection of the original data on the first 9 eigenvectors of Figure 9 are shown.*

### [redacted]Lock In Thermography

Following the scheme shown in Figure 1, the lamps are supplied by a power thyristor unit Eurotherm 7100, driven by a NI 6110 general purpose I/O box connected to a computer by USB. The typical temperature profile collected by the IR camera and processed by FFT, is shown in Figure 11 for a sound area (blue color) and a defected one (red color). Amplitude profile shows 2 major peaks in correspondence of the period of the modulation (16 sec) and some smaller peaks in correspondence of the 2nd, 3rd and 4th harmonic components. Lock In Thermography is supposed to give a better Signal To Noise Ratio than Pulse Thermography as the energy of the signal is concentrated in a single frequency. On the other hand it is considered less productive as different experiment (at different frequencies) must be carried out to probe the material at different depths.

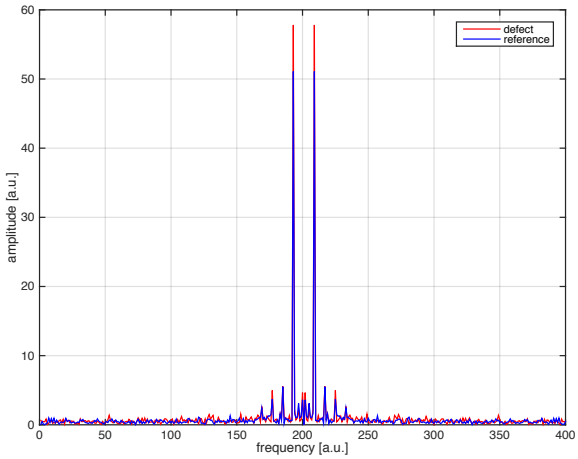


*Fig. 11. FFT of the temperature signal modulated with a period of 16 sec. Two major peaks are visible at ± the principal modulating frequency and some much smaller at the 2nd, 3rd and 4th harmonic components. The blue line corresponds to the non-defect zone and the red line to the defect one.*

By processing each pixel in the sequence of images the maps shown in Figure 12 are obtained. The amplitude at the period of 16 sec and the corresponding phase are shown.

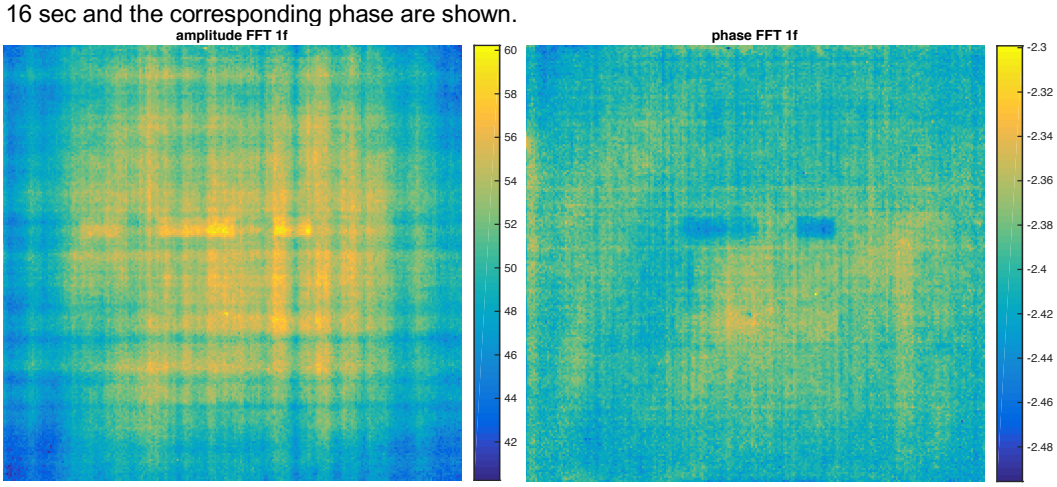


*Fig. 12. Amplitude (left) and phase (right) obtained after processing each pixel in the IR sequence by FFT.*

### Frequency modulated thermography

In this case the lamps are modulated with a period that is varying during the experiment. The advantage of this technique is that of being more productive than a pure LIT as in the single experiment a range of frequencies is utilized that allows to test a range of depths in the material under test. For this reason it can be considered as a compromise between Pulse Thermography and Lock In Thermography. The processing technique produce a correlation sequence between sound and defect areas and a phase sequence as well in time domain. The signal for sound (reference) and defect zone, are shown in Figure 13, while the correlation and phase are shown in Fig. 14.

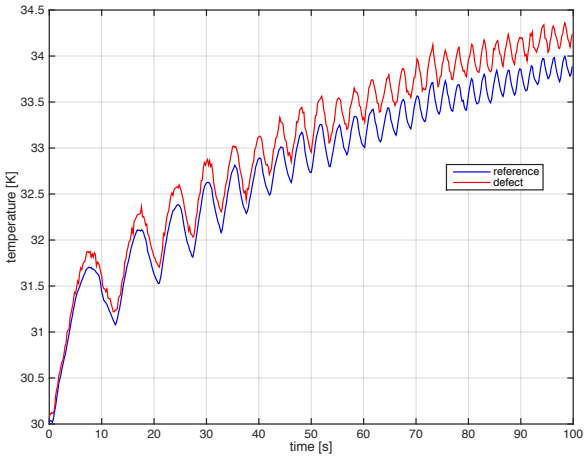


*Fig. 13. Temperature profile for sound (blue) and defect (red) zones. The initial period is 16 sec and the final is 2 sec.*

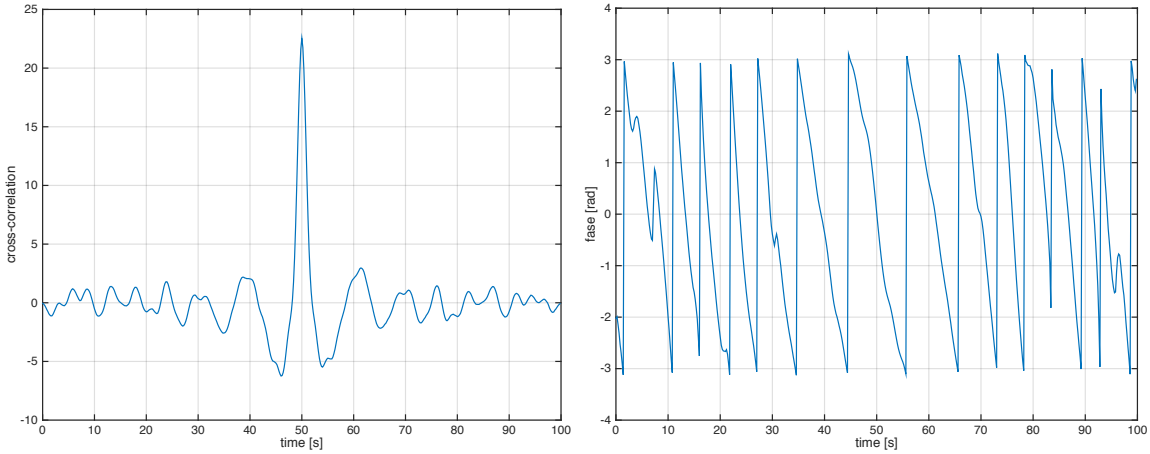


*Fig. 14. Correlation and phase in time domain obtained by processing the original signal shown in Fig. 13.*

By processing each pixel in the sequence of images the maps shown in Figure 15 are obtained.

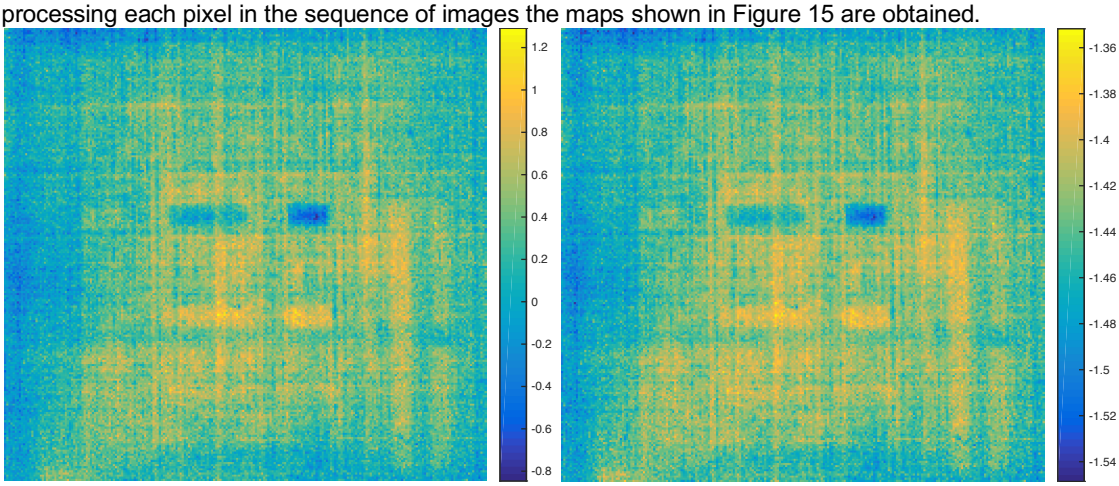

*Fig. 15. Maps of the correlation and phase obtained after processing the data of the experiment of Frequency Modulated Thermography.*

## 4. Conclusion

Three types of heating function have been applied to a sample of CFRP with artificial defects inside. The algorithm utilized to process the data have been described and the results obtained have been shown. The next step will be the comparison of such results by means of the evaluation of the percentage of the detected true positive at the expense of the percentage of false alarms.

## REFERENCES

[1] X. Maldague and S. Marinetti. Pulse phase infrared thermography. Journal of Applied Physics, 79(5):2694–2698, 1996.

[2] N. Rajic. Principal component thermography for flaw contrast enhancement and flaw depth characterisation in composite structures. Composite Structures, 58(4):521–528, 2002.

[3] S. Shepard, J. Lhota, B. Rubadeux, D. Wang, and T. Ahmed. Reconstruction and enhancement of active thermographic image sequences. Opt. Eng., 42(5):1337–1342, May 2003.

[4] V. Vavilov. Dynamic thermal tomography: Perspective field of thermal ndt. In S. A. Semanovich, editor, THERMOSENSE XII, volume 1313, pages 178–182. SPIE, 1990.

[5] G. Busse, D. Wu, and W. Karpen. Thermal wave imaging with phase sensitive modulated thermography. Journal of Applied Physics, 71:3962–3965, 1992.

[6] J. Krapez. Compared performances of four algorithms used for modulation thermography. In QIRT-1998, 1998.

[7] W. Winfree and K. Cramer. Computational pulse shaping for thermographic inspection. In D. Burleigh and J. Spicer, editors, Thermosense XVIII, volume 2766, pages 228–235, 1996.

[8] V. Vavilov and X. Maldague. Optimization of heating protocol in thermal ndt, short and long heating pulse: a discussion. Research in Nondestructive Evaluation, 6(1):1–18, 1994.

[9] S. Tuli and R. Mulaveesala. Defect detection by pulse compression in frequency modulated thermal wave imaging. QIRT Journal, 2(1):41–54, 2005.

[10] R. Mulaveesala and E. Tuli. Theory of frequency modulated thermal wave imaging for nondestructive subsurface defect detection. Applied Physics Letters, 89:191313–1 191313–3, 2006.

[11] A. Mandelis. Frequency modulated (fm) time delay photoacoustic and photothermal wave spectroscopies. technique, instrumentation, and detection. part i: Theoretical. Review of Scientific Instruments, 57:617– 621, 1986.

[12] A. Mandelis. Thermophotonic radar imaging: An emissivity-normalized modality with advantages over phase lock-in thermography. Applied Physics Letters, 98:163706–1 – 163706–3, 2011.

[13] P. Bison, A. Bortolin, G. Cadelano, G. Ferrarini, L. Finesso, "COMPARISON OF HEATING METHODS IN ACTIVE IR THERMOGRAPHY." ICPPP 18, Novi Sad, 2015, http://www.icppp18.com/predavaci.php - oral

[14] R. Barker. Group synchronizing of binary digital sequences. Communication Theory, pages 273–287, 1953.

[15] G. Silipigni, P. Burrascano, D. A. Hutchins, S. Laureti, R. Petrucci, L. Senni, L. Torre, M. Ricci," Optimization of the pulse-compression technique applied to the infrared thermography nondestructive evaluation." NDT&E International 87 (2017) 100–110.

[16] T. Fawcett. An introduction to roc analysis. Pattern Recognition Letters, 27:861–874, 2006.